remote sensing

MDPI

Article

Identification of Hazard and Risk for Glacial Lakes in the Nepal Himalaya Using Satellite Imagery from 2000–2015

David R. Rounce [1,*], C. Scott Watson [2] and Daene C. McKinney [1]

[1] Center for Research in Water Resources, University of Texas at Austin, Austin, TX 78758, USA; daene@aol.com

[2] School of Geography and water@leeds, University of Leeds, Leeds LS2 9JT, UK; gy09csw@leeds.ac.uk

* Correspondence: david.rounce@utexas.edu

Academic Editors: Qiusheng Wu, Charles Lane, Melanie Vanderhoof, Chunqiao Song, Deepak R. Mishra and Richard Gloaguen

Received: 19 April 2017; Accepted: 21 June 2017; Published: 26 June 2017

Abstract: Glacial lakes in the Nepal Himalaya can threaten downstream communities and have large socio-economic consequences if an outburst flood occurs. This study identified 131 glacial lakes in Nepal in 2015 that are greater than 0.1 km^2 and performed a first-pass hazard and risk assessment for each lake. The hazard assessment included mass entering the lake, the moraine stability, and how lake expansion will alter the lake's hazard in the next 15–30 years. A geometric flood model was used to quantify potential hydropower systems, buildings, agricultural land, and bridges that could be affected by a glacial lake outburst flood. The hazard and downstream impacts were combined to classify the risk associated with each lake. 11 lakes were classified as very high risk and 31 as high risk. The potential flood volume was also estimated and used to prioritize the glacial lakes that are the highest risk, which included Phoksundo Tal, Tsho Rolpa, Chamlang North Tsho, Chamlang South Tsho, and Lumding Tsho. These results are intended to assist stakeholders and decision makers in making well-informed decisions with respect to the glacial lakes that should be the focus of future field studies, modeling efforts, and risk-mitigation actions.

Keywords: glacial lake; Nepal; risk; hazard; downstream impact; avalanche; rockfall; moraine stability; lake expansion

1. Introduction

The Nepal Himalaya is home to a large number of glacial lakes that can be a serious threat to downstream communities if a glacial lake outburst flood (GLOF) occurs. GLOFs refer to the sudden release of stored lake water, which can have devastating socio-economic consequences, including loss of life, buildings, bridges, transportation routes, arable land, and hydropower systems. In the Himalaya, the main trigger of GLOFs is an avalanche entering a lake, which may cause a tsunami-like wave, that can overtop and erode the terminal moraine, and generate the ensuing flood [1–4]. Other secondary trigger mechanisms include displacement waves from rockfalls, moraine failure due to dam settlement and/or piping, the degradation of an ice-cored moraine, seismic activity, or the rapid input of water from extreme events or from an outburst flood from a glacial lake located upstream [1–5]. Often the unpredictable nature of these GLOFs and their remote locations make it difficult to determine the exact trigger and cause of failure, especially when one considers that these triggering mechanisms may be interconnected [4]. Nonetheless, quantifying the threat posed by these various triggering mechanisms is important, particularly in Nepal. A recent study found that Nepal is one of two countries that have the greatest socio-economic consequences from glacier outburst floods in the world [6]. The GLOFs that

occurred at Nare Lake in 1977 [7], Dig Tsho in 1985 [8], Tam Pokhari in 1988 [9], and Chubung lake in 1991 [10] are examples of the devastating socioeconomic impacts that can be caused by GLOFs, which include loss of life in addition to damage to livelihoods, hydropower systems, and infrastructure.

In recent years, the proliferation of open access satellite imagery has made it possible to monitor changes in glacial lakes. Regional studies have found that glacial lakes in Nepal are among those experiencing the most rapid growth in the Himalayas from 1990 to 2009/15 (Table 1) [11–14]. Of these lakes, proglacial lakes have been experiencing the most rapid expansion followed by supraglacial lakes [11–13] due to their connection to their parent glaciers, which provide opportunities for these lakes to grow via calving retreat [14,15]. Local studies have also investigated the temporal and spatial variability of supraglacial ponds in Nepal [16,17] in an effort to understand how these supraglacial ponds start to coalesce and form into larger proglacial lakes [18–20].

Table 1. Previous studies [11–14] that investigated regional trends of glacial lake expansion in Nepal.

Study	Region	Study Period	Lake Expansion
Gardelle et al. (2011) [11]	West Nepal Everest	1990–2000, 2000–2009 1990–2000, 2000–2009	+30%, +7% +13%, +20%
Nie et al. (2013) [12]	Central Himalaya	1990–010	+17%
Nie et al. (2017) [13]	Central Himalaya	1990–2015	+23%
Song et al. (2017) [14]	Himalayas (>0.5 km^2)	2000–2014	+37%

Regional surveys provide initial data that enable hazard and risk assessments to be performed. Regional hazard assessments have been performed for the southeastern Tibetan Plateau [2], the Chinese Himalaya [21], Uzbekistan [22], Nepal [23,24], Bhutan [25], India [26,27], and the entire Himalayas [28]. The major differences between these studies have been the parameters used and the weight/importance given to each parameter. Rounce et al. (2016) [29] focused on eight glacial lakes in Nepal and found that the use of various parameters and weights led to highly conflicting classifications of hazard. These conflicting classifications can cause confusion among the stakeholders who these studies are meant to assist. Therefore, it is important for these hazard assessments to be both holistic, i.e., account for the various trigger mechanisms, and developed in an objective manner that can help stakeholders identify the lakes that require further investigation.

The aim of this study is to conduct a holistic hazard and risk assessment of all the glacial lakes in the Nepal Himalaya. To accomplish this goal, a remote sensing glacial lake survey for the Nepal Himalaya was performed for 2000 and 2015 using Landsat satellite imagery. Next, a hazard assessment that accounts for mass entering the lake and the moraine stability was conducted. A geometric GLOF model was then applied to each lake in order to quantify the potential downstream impacts. Finally, the hazard and downstream impact were combined in order to prioritize the glacial lakes according to their risk with the overall objective of providing actionable conclusions for the stakeholders in Nepal to guide more detailed investigations of the lakes identified as particularly dangerous.

2. Methods

2.1. Glacial Lake Survey

Every lake in Nepal that was greater than 0.1 km^2 and located less than 10 km from a glacier was considered in this study (Figure 1). The minimum lake area of 0.1 km^2 was selected based on the minimum lake size that Wang et al. (2012) [21] determined based on nineteen moraine-dammed lake outburst floods in the Tibetan Plateau, which is also consistent with the GLOFs from Dig Tsho [8] and Tam Pokhari [9] in Nepal. The 10 km threshold [13] was used in order to maximize the number of lakes included in this study that may be potentially affected by glacier hazards. Since glacial lakes in Nepal have been experiencing some of the highest growth rates in the Himalayas (Table 1) [11–14], Landsat satellite imagery was used to delineate each lake in the fall of 2000 and 2015 in order to quantify lake

area and expansion rates. An exception was made for two lakes, which required imagery from the fall of 1999 due to cloud coverage.

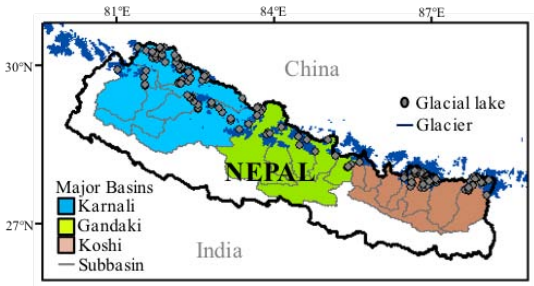

Figure 1. Study area showing glacial lakes and glaciers in Nepal along with major basins and subbasins adapted from ICIMOD (2011) [24].

Lake delineations were performed using the normalized difference water index (NDWI) [30–32], which is a combination of the near-infrared and blue bands. NDWI thresholds were manually selected based on the contour that provided the best delineation of the lake based on the panchromatic band of Landsat 7 and 8, which has a resolution of 15 m. For five lakes, heavy shadows from the surrounding topography prevented the use of NDWI contours, so these lakes were manually delineated using the panchromatic band. The uncertainty associated with all lake delineations was assumed to be half a pixel multiplied by the perimeter of lake [32]. Significant drainage or growth was defined as a change in lake area between 2000 and 2015 that exceeded the error associated with the 2015 delineation.

For lakes that experienced significant growth, their future areal extents for 2030 and 2045 were projected using their 15-year expansion rate along with ice thickness estimates from the GlabTop2 model [33] in order to determine how lake growth may alter the lakes' proximity to future hazards. Specifically, the ice thickness estimates were used to model overdeepened areas of the glacier to identify areas where glacial lakes could potentially expand to in the future as previously done in this region [34]. The glacial lakes were assumed to grow at a linear rate based on the expansion rates from 2000–2015 in order to estimate the areal extents in 2030 and 2045. Rounce et al. (2016) [29] analyzed the annual change in areal extent of three glacial lakes in Nepal that experienced significant growth (Imja Tsho, Lower Barun Tsho, and Lumding Tsho), which suggested that the assumption of a linear rate of expansion is reasonable (R^2 values ranged from 0.96–0.99). Actual future extents will be effected by the accuracy of the glacier outlines and ice thickness estimates, in addition to the lake-glacier dynamics and climatic forcings. The uncertainty associated with the glacier outlines used in this study is estimated to be ~15% [35], although the uncertainty of debris-covered glaciers can be up to 30% [36]. The uncertainty associated with the ice thickness estimates are ±30% [33,34].

Lake type was classified as proglacial, supraglacial, unconnected glacier-fed, and unconnected, non-glacier-fed [13]. Glacier outlines from the Randolph Glacier Inventory Version 5.0 [35,37] and ice thickness data [33] were used to differentiate between unconnected and connected glacial lakes. These glacier outlines are based on satellite imagery from 1999–2003 [35]. Supraglacial lakes were considered to be any connected glacial lake that had ice present down-glacier.

2.2. Hazard Parameters

The remote hazard assessment models ice avalanche trajectories, landslides/rockfalls, upstream GLOFs, and moraine stability using the same criteria as Rounce et al. (2016) [29] with minor adjustments. Hazards related to mass entering the lake are referred to as dynamic failures, while hazards related to the failure of the moraine via hydrostatic pressure, a buried ice core, or time are referred to as self-destructive failures [3,38]. A brief overview of the methods used to assess each parameter and specific details of the adjustments to Rounce et al. (2016) [29] are described below.

The Randolph Glacier Inventory Version 5.0 [35,37] was used in conjunction with the 30 m ASTER GDEM V2 [39], hereon referred to as GDEM, in order to identify avalanche prone areas, i.e., any glacier area with a slope between 45–60° [9,40,41]. Glacier outlines were used instead of the NIR/SWIR band ratio that was used by Rounce et al. (2016) [29] in order to provide a consistent product over the entire study area that was not affected by seasonal snow. These glacier outlines are subject to uncertainties associated with the delineation of clean ice, which can have errors of ~5% of the glacier area [36]. Furthermore, the avalanche model assumes avalanche depths of glacier ice of 10 m, 30 m, and 50 m. These avalanche depths are realistic for glacier ice thickness derived from the relationship between thickness, shear stress, slope factor, and slope [21], and are also similar to those that have previously been observed in the European Alps and Russia [42,43].

Maximum avalanche prone area was computed using a variable kernel filter with a 100% threshold, i.e., a 1 × 1 pixel grid is assessed to determine if all pixels are prone, which is then expanded to a 2 × 2 pixel grid, etc., until the grid fails to meet the threshold. The maximum avalanche prone area is combined with the assumed avalanche thickness to determine avalanche volume. Avalanche prone areas that were less than 0.1 million cubic meters (mcm) were discarded. This was the minimum size avalanche that Richardson and Reynolds (2000) [1] defined as large or extreme snow and ice avalanches, which have the potential to cause general and widespread destruction. Furthermore, the GLOF at Dig Tsho in 1985 was triggered by an ice avalanche that was ~0.15 mcm [8]. Additionally, GLOF modeling studies that model an ice avalanche, the wave propagation, the overtopping/erosion of the moraine, and the downstream flood have found that avalanches larger than 0.5 mcm are required to cause a GLOF for a dangerous glacial lake in the Indian Himalaya [44], and another lake in Cordillera Blanca [44,45]. Avalanche volume was used to estimate the average trajectory slope, i.e., the average angle between the starting zone and the furthest point of deposition, according to Huggel et al. (2004) [42]:

$$\tan(\alpha) = 1.111 - 0.118 \log(V) \quad (1)$$

where α is the average trajectory slope (°), hereon referred to as the average "look-up" angle, and V is the avalanche volume (m^3). A minimum threshold of 17° was used, since avalanches rarely exceed this average "look-up" angle [42]. The avalanche trajectory was then modeled using the flow direction algorithm in ArcGIS 10.3 with a sink-free GDEM such that the avalanche stopped once the "look-up" angle was reached [42]. A sensitivity test was conducted to determine the effect of altering the "look-up" angle by ±3°.

Rockfalls were similarly modeled for rockfall prone areas, which were considered to be non-glacier regions with a slope greater than 30° [46]. Rockfall prone areas were computed using the same variable kernel filter with a 100% threshold, which was combined with an assumed thickness to determine rockfall volume. Rockfall thickness was assumed to be 4 m based on previous studies in the Nepal Himalaya that found landslides and major rock slides are typically less than 4 m [47,48]. Rockfall volumes less than 0.1 mcm were discarded as described above. Rockfall trajectories were modeled until an average "look-up" angle of 20° was reached [47]. Again, a sensitivity test was conducted to determine the effect of altering the "look-up" angle by ±3°.

Upstream GLOFs, i.e., outburst floods sourced from glacial lakes that are located upstream of the lake and have the ability to cause a cascade of GLOFs, were modeled using the Monte-Carlo Least Cost Path (MC-LCP) model [49] (see Section 2.3). Any glacial lake that was greater than 0.05 km^2 and upstream of a glacial lake was modeled as a potential upstream GLOF as complete drainage of these lakes could cause ~0.5 mcm of water to enter a glacial lake, which is the same order of magnitude as the smallest avalanches considered (0.27 mcm).

Moraine stability was assessed using a combination of the average angle of the steep lakefront area (SLA) [28] and the potential for an ice-cored moraine based on the presence of supraglacial ponds and/or changes in the outlet channel [29]. A threshold angle of 10° was used for the SLA angle [28] to determine if the moraine was stable or unstable. Google Earth and Landsat images were used to

identify ponds on the terminal moraine and/or changes in the outlet structure, e.g., a change in the location of the outlet.

2.3. Downstream Impacts

A GLOF from each glacial lake was modeled using the MC-LCP model [49] with the unmodified GDEM [39]. The MC-LCP model is a first-pass GIS-based GLOF assessment that incorporates an iterative cost path analysis and Monte Carlo loop of modeled DEM uncertainty to estimate GLOF extents [49]. Since the model does not require a 'filled' DEM, it is particularly suited for high-relief topography where large artefacts may be present in coarse resolution DEM products. The MC-LCP model with the GDEM at 30 m resolution was found to generate a conservative flood extent when compared to the flood extent from Dig Tsho in 1985 [49] and the modeled extent of a 33.5 mcm flood volume from Imja Tsho [29,50]. A cutoff distance of 50 km downstream was applied to each MC-LCP model in order to facilitate a standardized comparison of the downstream impacts between various lakes. The distance of 50 km was selected based on the GLOF at Dig Tsho, which was found to significantly erode material as far as 42–90 km downstream [1,8]; however, the GLOF at Luggye Tsho in Bhutan in 1994 showed that the flood wave may still be sizeable (~2 m) up to 200 km downstream [1,51].

The GLOF extents were used to quantify the number of buildings, bridges, agricultural land, and hydropower systems, as of January 2015, that were in the path of a potential GLOF. The locations of buildings were downloaded from OpenStreetMap (@OpenStreetMap contributors, West Midlands, UK, https://www.openstreetmap.org/) and Google Earth was used to validate and update the data set where required. The updates to the OpenStreetMap data set were particularly important for accurately quantifying the potential inundation of buildings in eastern and western Nepal, where the number of buildings was greatly underrepresented. A total of 7447 buildings were added to the original dataset. Bridges were mainly identified in GoogleEarth imagery, but were also identified as any road/path from OpenStreetMap that crossed the river. Agricultural land located within the flood extent was identified using a 2010 land cover map of Nepal [52], which was validated in Sagarmatha (Mount Everest) National Park [53]. Lastly, the number of hydropower systems that could be affected by a GLOF was estimated using an inventory from the Government of Nepal's Department of Electricity Development (http://www.doed.gov.np/operating_projects_hydro.php, retrieved on 13 February 2017) in addition to a shapefile that accompanied ICIMOD (2011) [24]. A hydropower system that could be affected was considered to be any system that was within 1 km of the flood extent, since preliminary results revealed that only one hydropower system point intersected the flood extents, despite knowledge of other hydropower systems that would be threatened by GLOFs (e.g., Tsho Rolpa). This discrepancy was likely caused by the hydropower system point being placed in a location that was generally representative of the system, but not necessarily specific parts of the system like the intake, which are connected to the river.

The potential flood volume (PFV) for each GLOF was estimated for both self-destructive and dynamic failures. For self-destructive failures associated with unstable moraines, the approach from Fujita et al. (2013) [28] for calculating the PFV was adopted; however, the mean depth and lake volume equations were based on the revised fit of Huggel et al. (2002) [54] by Cook and Quincey (2015) [55], i.e., the mean depth was estimated as

$$D = 0.1217A^{0.4129}, \quad (2)$$

where D is the mean depth (m) and A is the 2015 lake area (m^2) and the relationship for volume (m^3) was

$$V = 0.1217A^{1.4129}. \quad (3)$$

These equations were used such that the mean depths were more realistic as opposed to the maximum mean depths that were used by Fujita et al. (2013) [28], which provided much more conservative estimates of PFV such that the PFV was found to exceed the estimated lake volume in some cases (e.g., Tsho Rolpa). The use of these equations, which linked the mean depth to the lake

volume, ensured that the PFV was always less than or equal to the lake volume. For dynamic failures, which include any form of mass entering the lake, the PFV was estimated using the assumption that the mass entering the water displaces potential flood water at a 1:1 ratio. For lakes that were threatened by an upstream GLOF, the PFV was assumed to be equal to the maximum PFV associated with the upstream lake. The maximum PFV for each lake was the maximum PFV associated with either a self-destructive or dynamic failure.

2.4. Classification of Hazard, Downstream Impacts, and Risk

Since the aim of this study is to assess the hazard and risk associated with glacial lakes, a framework was developed to transform the parameters and impacts into a ranking of hazard, downstream impacts, and risk. Initially, the framework from Rounce et al. (2016) [29] was applied; however, there was an uneven distribution of lakes classified as very high, high, moderate, and low. This uneven distribution effectively eliminated entire sections of the risk chart (Figure 2), which made it more difficult to identify lakes that were more dangerous and should be the priority of further investigations (see Results). Therefore, the framework used to compute the hazard, downstream impact, and risk was adjusted in an effort to develop a classification system that can be used to prioritize the lakes that are the highest risk in Nepal. As this portion of the study is inherently subjective, decisions were made based on the main triggers of previous GLOFs and applying thresholds that improved the overall distribution of lakes that were classified as very high, high, moderate, and low for the hazard, downstream impacts, and risk. Specifically, improvements to the distribution were considered to be changes that distributed the lakes more evenly over the four classifications (very high, high, moderate, and low) as this effectively utilizes all of the risk chart (Figure 2).

The framework for classifying the lake hazard (Figure 2) was adapted from Rounce et al. (2016) [29] and includes two modifications. The first modification is that very high hazard lakes are those susceptible to an avalanche entering the lake and have a steep (>10°) moraine. This was given the highest ranking of very high hazard to reflect the two most common triggering mechanisms, i.e., an avalanche entering the lake and an unstable moraine [1,3,4]. High hazard is any lake that may have an avalanche entering the lake or a lake that has a steep moraine most likely with an ice core. The combination of a steep moraine with an ice-cored moraine was given a higher rating than solely a steep moraine, since an ice-cored moraine can cause piping failure and/or affect dam settlement. The second modification to Rounce et al. (2016) [29] is that a lake susceptible to a rockfall or a GLOF from an upstream lake is given a moderate hazard without any additional modification. This change was made to reflect that there have only been two documented GLOFs triggered by a rockfall [1,3]. Moderate hazard also includes any lake that has a steep moraine without an ice core. Lastly, low hazard is considered to be any lake that is not susceptible to any form of mass entering the lake and has a gentle moraine (<10°).

The classification of downstream impacts was adapted from Rounce et al. (2016) [29] with one minor modification. Very high downstream impact is considered to be any lake that threatens a hydropower system and a large number of buildings, i.e., more than 20 buildings. The use of a "large" number of buildings is the one modification made to Rounce et al. (2016) [29], which is based on the distribution of buildings that could be affected by a flood (see Results) and is meant to distinguish between downstream impacts that would affect large numbers of buildings compared to a relatively small number of buildings. Furthermore, this distinction greatly improves the distribution of lakes in each classification. High downstream impact is any lake that threatens a hydropower system or a large number of buildings. Moderate downstream impact is any lake that threatens a small number of buildings, bridges, or agricultural land, and low downstream impact is no effect on human activity.

The classification of risk (Figure 2) was also slightly modified from Rounce et al. (2016) [29] and Worni et al. (2013) [26] such that any combination of high hazard and very high downstream impact or vice versa is defined as very high risk. Again, this modification was made to improve the distribution of lakes in each category, since initial results revealed that no lakes were classified as very high risk

based on the framework from Rounce et al. (2016) [29], i.e., no lakes were both very high hazard and very high downstream impacts (see Results).

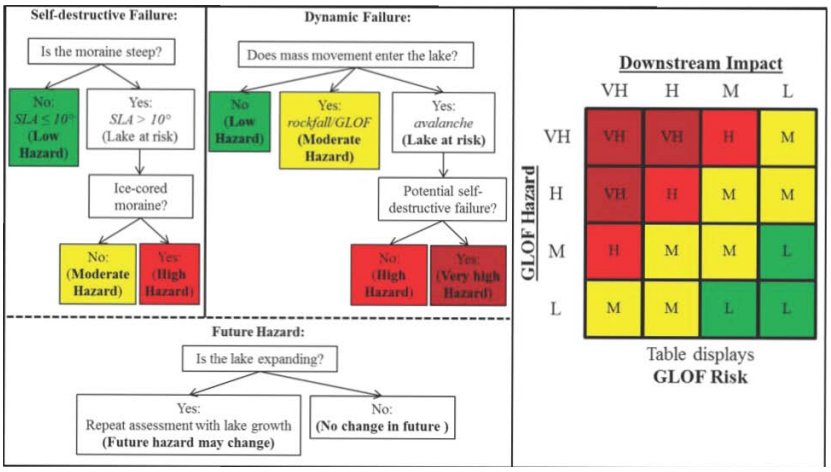

Figure 2. Hazard classification flow chart for dynamic and self-destructive failures and the GLOF risk chart as a function of hazard and downstream impacts.

3. Results

3.1. Glacial Lake Survey

In 2015, 131 lakes greater than 0.1 km^2 were identified, which covered a total area of 41.3 ± 4.9 km^2. The lake size distribution (Figure 3) reveals that 94 (72%) of the lakes were less than 0.25 km^2, 23 (18%) were less than 0.5 km^2, and only 14 (11%) were greater than 0.5 km^2. According to lake type, unconnected glacier fed lakes accounted for 64 lakes (49%), followed by 37 proglacial lakes (28%), 24 non-glacier-fed lakes (18%), and 6 supraglacial lakes (5%). The elevation of these lakes ranged from 3572 m.a.s.l. to 5723 m.a.s.l. with an average elevation of 4837 m.a.s.l. The lakes that were located below 4500 m.a.s.l. were predominantly unconnected glacier-fed and non-glacier-fed lakes, while above 4500 m.a.s.l. there was an increase in proglacial lakes and glacier-fed lakes and a decrease in non-glacier-fed lakes. The distance to glacier distribution (Figure 3) shows that 66 (50%) of the lakes are located within 0.5 km from a glacier and only 13 (10%) of the lakes are located further than 3 km from a glacier. In 2000, these lakes covered a total area of 37.8 ± 4.5 km^2, which revealed that these lakes grew by 9.2% in 2015 with proglacial lakes accounting for 81.2% of the total growth. During this time, 22 lakes significantly expanded and 6 lakes significantly drained.

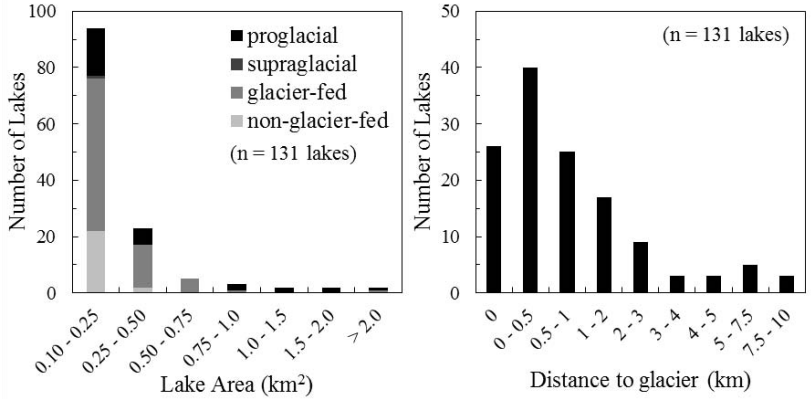

Figure 3. Distribution of lake size according to lake type and the distance to glacier for all lakes in Nepal.

3.2. Hazard

The hazard assessment modeled avalanches, rockfalls, upstream GLOFs, moraine stability, and the presence of an ice core. For avalanches and rockfalls, the angle of the trajectory was also considered based on the starting point of the mass movement and the aspect of the lake; specifically, a direct hit was considered to be any trajectory who's starting point is within ±45° of the lake's major axis, which could have important implications for wave run-up and moraine overtopping. With respect to dynamic failures for the 131 lakes, 32 (24%) were susceptible to an avalanche entering the lake, 105 (80%) were susceptible to a rockfall entering the lake, and 26 (20%) were susceptible to an upstream GLOF (Figure 4). Only 8 of the 32 lakes (25%) that were susceptible to an avalanche were susceptible to a direct hit, and 29 of the 105 lakes (28%) that were susceptible to a rockfall were susceptible to a direct hit, which revealed that most avalanches and landslides were entering the lakes along their minor axes. With respect to self-destructive failures for the 131 lakes, 87 (66%) had an unstable moraine, i.e., an average SLA angle greater than 10°, and 32 (24%) potentially had an ice core (Figure 4).

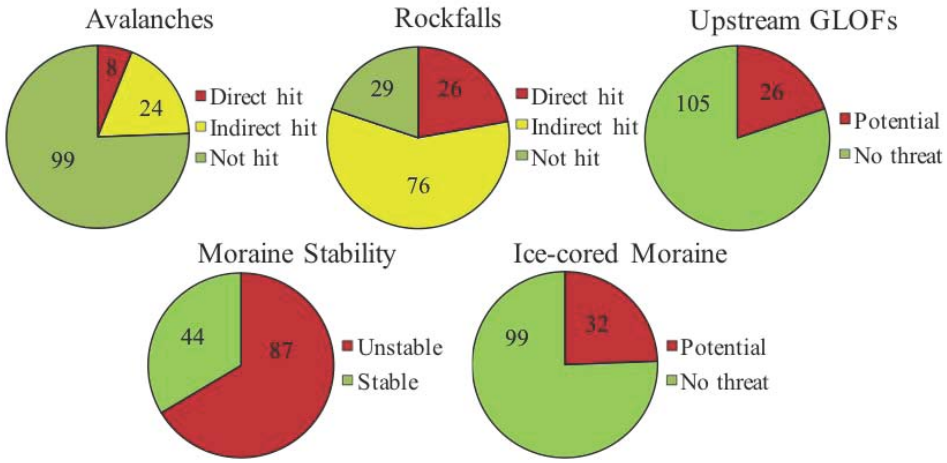

Figure 4. Breakdown of hazard parameters that threaten the glacial lakes.

The hazard parameters were used to classify the hazard associated with each lake (Figure 2), which resulted in 19 lakes being classified as very high hazard, 26 as high, 82 as moderate, and 4 as low (Figure 5). The Koshi basin had the greatest number of very high hazard lakes (10 lakes) followed by the Karnali basin (6 lakes) (Figure 5). Lake type appeared to influence the hazard classifications as 59% of proglacial lakes were classified as high or very high hazard compared to 33%, 25%, and 21% for supraglacial, glacier-fed, and non-glacier-fed lakes, respectively. This is likely due to the connection between proglacial lakes and their parent glacier, which makes these lakes more susceptible to avalanches. There were no apparent trends between hazard and lake elevation.

The commonly known very high hazard lakes were Chamlang North Tsho, Chamlang South Tsho, Lumding Tsho, and Phoksundo Tal. Well-studied lakes such as Tsho Rolpa (high hazard), Thulagi Tsho (moderate hazard), and Imja Tsho (moderate hazard) were not considered to be very high hazard due to the lack of avalanche trajectories that could enter the lake. For the 22 lakes that experienced significant growth, only seven of these lakes had the ability to expand based on the bedrock topography derived from the GDEM [39] and ice thickness data [33]. For these seven lakes, the hazard classification of only one (Imja Tsho) changed from moderate to high due to the potential for an avalanche to enter the lake in the future. One other lake (Barun Tsho) had an increase in the number of avalanches that could potentially enter the lake, but its hazard did not change because they were already susceptible. The hazard associated with the other five lakes did not change.

For avalanches, the sensitivity test of changing the "look-up" angle threshold by ±3° did not alter the hazard ratings. For rockfalls, a decrease in the "look-up" angle threshold to 17° caused

four additional lakes to be susceptible to rockfalls, which altered the hazard classification of three of those four lakes from low to moderate. An increase in the "look-up" angle threshold to 23° caused seven lakes to no longer be susceptible to rockfalls, which altered the hazard classification of two of those lakes from moderate to low. Given the uncertainties associated with the volume and trajectories of the avalanches and rockfalls, the effect that the "look-up" angle has on hazard classifications is considered to be minimal.

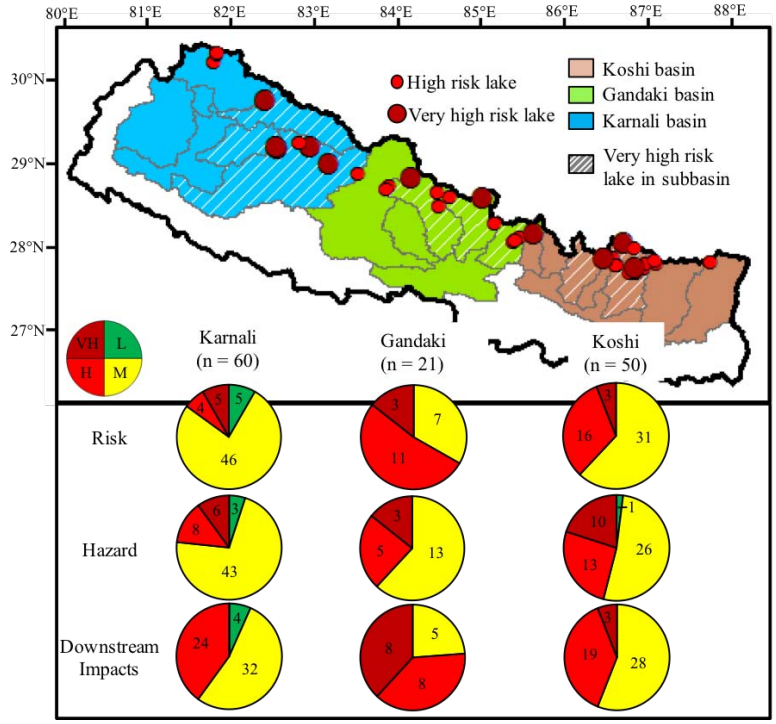

Figure 5. Distribution of risk, hazard, and downstream impacts classifications (pie charts) for each basin. The map shows all lakes classified as very high or high risk with hatched lines showing a sub-basin that has at least one lake classified as a very high risk.

3.3. Downstream Impacts

The MC-LCP model was used to quantify the buildings, hydropower systems, agricultural land, and bridges potentially inundated by a GLOF from each lake. Figure 6 shows 121 (92%) of the lakes inundated at least one building, while 64 (49%) of the lakes inundated at least 20 buildings. The number of buildings inundated varied from 0 to 634 with a median of 17 buildings. The number of hydropower systems threatened was much lower with only 11 (8%) of the lakes threatening a hydropower system. The amount of agricultural land inundated varied greatly from 0 to 4.5 km^2 with a median of 0.26 km^2, and the number of bridges varied from 0 to 25 with a median of 4.

Based on the downstream impact ranking system using a threshold of 20 buildings to differentiate between a large and small number of inundated buildings, 11 lakes were classified as very high downstream impacts, 51 as high, 65 as moderate, and 4 as low. If the threshold of 20 buildings was not applied, as in Rounce et al. (2016) [29], then 110 lakes would be classified as high and only 6 lakes would be classified as moderate. The differences in the classifications shows that the 20 building threshold helps to distribute the downstream classifications of high and moderate with 64 (49%) of the lakes potentially inundating a "large" number of buildings and 67 (51%) of the lakes potentially inundating a smaller number of the buildings. Adjusting the number of buildings by ±5 alters the downstream impacts classification of 6–8 lakes. All 11 lakes that threatened a hydropower system also inundated more than 20 buildings, so they were all classified as very high downstream impacts. This illustrates that hydropower systems appear to be located near the communities who will consume the electricity

generated. Regionally, the highest downstream impacts occur in the Gandaki basin with 8 very high downstream impacts lakes followed by the Koshi basin with 3 (Figure 5). Commonly known lakes with very high downstream impacts were Tsho Rolpa and Thulagi Tsho.

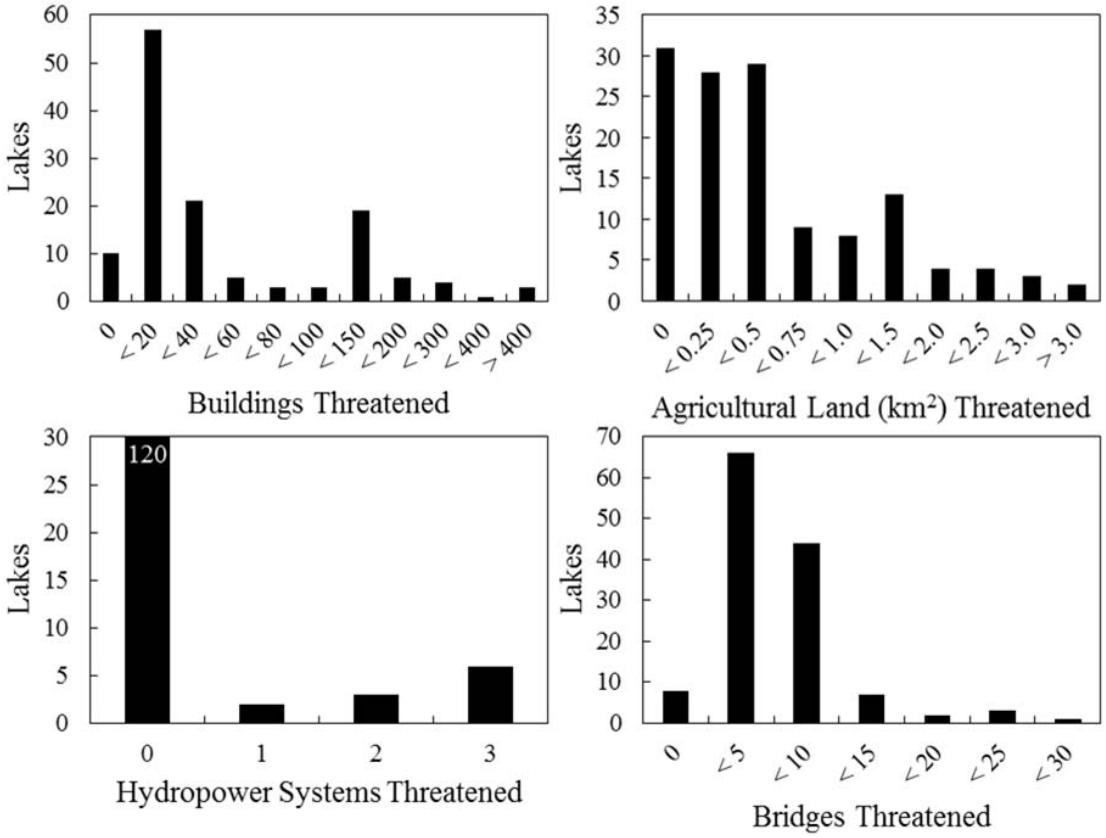

Figure 6. Summary of downstream impacts showing the number of buildings, agriculture (km^2), hydropower systems, and bridges threatened by GLOFs.

3.4. Risk

Initially, the hazard, downstream impact, and risk framework from Rounce et al. (2016) [29] was applied, which classified 0 lakes as very high risk, 60 as high, 64 as moderate, and 7 as low. This unbalanced distribution with 60 high risk lakes and 64 moderate risk lakes made it difficult to interpret the results of the risk assessment in a manner that would allow the lakes with the greatest risk to be prioritized. Specifically, it is impractical to suggest further investigation of 60 lakes. Hence, the framework from Rounce et al. (2016) [29] was modified for this study (see Methods). Based on this new framework, 11 lakes were classified as very high risk, 31 as high, 84 as moderate, and 5 as low.

Of the 11 lakes that were classified as very high downstream impacts, only two of them were classified as very high risk, while the other 9 lakes were classified as high risk due to their moderate hazard. The remaining 9 lakes that were classified as very high risk, were susceptible to an avalanche entering a lake with an unstable moraine (very high hazard) and could potentially inundate more than 20 buildings (high downstream impact). Regional trends reveal that the Karnali basin had the greatest number of very high risk lakes (5), and the Koshi basin had the greatest number of very high and high risk lakes (19) (Figure 5). Table 2 shows the hazard parameters, downstream impacts, and risk associated with the lakes that were identified by Mool et al. (2001) [23] and ICIMOD (2011) [24] as being a potential high hazard or risk of a GLOF. Out of the 24 lakes that were identified in these studies, this study classified 2 of these lakes as very high risk, 12 as high, 9 as moderate, and 1 was not a lake.

Table 2. Hazard parameters, downstream impacts, risk classification, and lake data associated for lakes that were identified by ICIMOD (2011) [24] and Mool et al. (2001) [23] as being potential high hazards. Hazard, downstream impact, and risk classification values refer to low (0); moderate (1); high (2); and very high (3). Ice core value of 1 indicates a potential ice core. Additional details on all lakes are provided in the Supplementary Materials (Table S1).

Lake Data							Classification			Hazard Data						Downstream Impacts			
This Study ID	ICIMOD (2011) ID	Common Name	Longitude (°)	Latitude (°)	Elev (m.a.s.l)	2015 Area (km^2)	Hazard	Impact	Risk	Max PFV (mcm)	Average SLA Angle (°)	Ice Core	Avalanche (mcm)	Rockfall (mcm)	Up-Stream GLOF (mcm)	Buildings	Bridges	Agriculture (km^2)	Hydropower Systems
54	kotak_gl_0009	Tsho Rolpa	86.477	27.862	4526	1.52	2	3	3	66.3	17.4	1	0.0	0.7	1.4	258	10	0.68	2
19	koaru_gl_0009	Barun	87.097	27.798	4535	1.64	2	2	2	1.5	7.2	1	0.7	0.7	1.5	33	4	0.76	0
25	kodud_gl_0184	Imja	86.923	27.899	4998	1.26	1	2	1	0.4	5.4	1	0.0	0.4	0.0	134	8	0.28	0
49	kodud_gl_0036	Lumding	86.614	27.779	4819	1.18	3	1	2	21.4	11.0	0	2.2	0.7	8.7	1	3	0.28	0
22	kodud_gl_0242	Chamlang South	86.960	27.755	4952	0.84	3	1	2	9.3	10.7	1	1.6	0.7	0.0	4	3	0.09	0
69	gamar_gl_0018	Thulagi	84.486	28.489	4009	0.88	1	3	2	0.7	6.5	1	0.0	0.7	0.0	267	25	0.95	3
6	kotam_gl_0135	Nagma	87.867	27.870	4945	0.65	1	1	1	0.7	10.4	0	0.0	0.7	0.0	3	6	0.43	0
21	kodud_gl_0241	Chamlang North	86.957	27.784	5218	0.86	3	1	2	29.6	19.4	0	0.7	0.7	0.0	4	3	0.03	0
-	kotam_gl_0191	-	-	-	-	-	-	-	-	-	-	-	-	-	-	-	-	-	-
79	gakal_gl_0004	-	83.528	28.888	5589	0.29	2	2	2	0.2	7.7	0	0.2	0.1	0.0	382	5	0.29	0
42	kodud_gl_0012	Seto/Barun Pohkari	87.082	27.845	4843	0.34	2	2	2	0.7	9.8	1	0.7	0.7	0.0	22	3	0.35	0
44	kodud_gl_0238	East Hongu 1	86.967	27.799	5402	0.21	1	1	1	2.6	7.3	1	0.0	0.4	2.6	4	3	0.03	0
68	gabud_gl_0009	-	84.630	28.597	3625	0.24	2	2	2	0.7	10.0	0	0.2	0.7	0.0	62	6	0.14	0
31	kodud_gl_0220	Mera	86.912	27.795	5238	0.17	2	1	1	2.4	12.4	1	0.0	0.0	0.0	4	3	0.03	0
20	koaru_gl_0016	Barun Upper Tsho	87.096	27.830	5245	0.11	1	2	1	1.5	14.9	0	0.0	0.4	0.0	22	3	0.44	0
82	gakal_gl_0008	-	83.673	29.046	5443	0.11	1	1	1	0.2	10.3	0	0.0	0.2	0.0	1	0	0.09	0
5	kotam_gl_0111	-	87.750	27.817	4935	0.16	3	1	2	2.7	19.5	0	0.2	0.5	0.0	14	8	0.40	0
38	kodud_gl_0239	East Hongu 2	86.975	27.806	5505	0.16	3	1	2	2.6	12.6	0	0.7	0.3	0.0	3	3	0.02	0
73	gakal_gl_0022	-	83.701	29.218	5427	0.42	1	1	1	0.2	1.7	0	0.0	0.2	0.2	2	4	0.00	0
77	gakal_gl_0023	-	83.682	29.201	5488	0.21	1	1	1	0.2	7.6	0	0.0	0.2	0.0	2	4	0.00	0
23	kodud_gl_0049	Dig Tsho	86.587	27.875	4367	0.38	2	2	2	0.7	9.0	0	0.4	0.7	0.0	137	3	0.39	0
41	kodud_gl_0193	-	86.845	27.743	4347	0.25	3	2	3	2.3	14.7	0	0.4	0.7	0.0	22	3	0.86	0
27	kodud_gl_0205	-	86.859	27.688	4762	0.28	3	1	2	6.0	20.4	1	0.4	0.5	0.0	17	5	1.04	0
43	kodud_gl_0229	Hongu 1	86.936	27.838	5217	0.23	2	1	1	4.6	14.5	1	0.0	0.2	12.7	3	3	0.01	0

4. Discussion

4.1. Glacial Lake Survey

The glacial lake survey agrees well with Nie et al. (2017) [13] who identified 127 lakes greater than 0.1 km^2 in Nepal in 2015 that had a total area of 36.9 km^2. The slight differences in lake number and total area are due to minor variations in lake delineations, which likely caused some lakes around 0.1 km^2 to not be included because they were below the threshold. The area of each lake from 2000 and 2015 was compared to Nie et al. (2017) [13], and comparisons were also made to ICIMOD (2011) [24] and Fujita et al. (2013) [28] for lakes that appeared stable, i.e., they did not experience significant growth or drainage between 2000 and 2015 (Supplementary Material, Table S2). The mean differences in lake area ranged from −0.024 to 0.007 km^2 for the four comparisons, which is well within the typical errors associated with lake delineations, which ranged from 0.018 km^2 to 0.259 km^2 with an average error of 0.037 km^2. This suggests that the method used to estimate lake area error [32], i.e., half a pixel multiplied by the lake perimeter, is quite reasonable.

One major difference between each study is the criteria that are used for including glacial lakes. This study used the criteria from Nie et al. (2017) [13], i.e., all glacial lakes within 10 km of a glacier, that are at least 0.1 km^2 [21]. Fujita et al. (2013) [28] limited their study to moraine-dammed glacial lakes, and ICIMOD (2011) [24] limited their study to all lakes above 3500 m.a.s.l. The maximum distance away from a glacier for lakes that were also assessed in this study was 5.6 km and 8.0 km for Fujita et al. (2013) [28] and ICIMOD (2011) [24], respectively. The main glacier hazard investigated in our study was an avalanche. The maximum distance that a lake was away from a glacier and was still susceptible to an avalanche entering the lake was 2.3 km. This suggests that ~2.5–3 km may be a good distance threshold for studies that are only focused on glacial lakes and/or glacier hazards. If a threshold of 3 km was used, 14 lakes would be removed from this study. The benefit of using a distance threshold when conducting the glacial lake survey is the inclusion of lakes is not affected by lake type, which can be subjective. This can be particularly problematic when differentiating between proglacial, supraglacial, and glacier-fed lakes, since current glacier outlines on debris-covered glaciers can differ by up to 30% of the glacier area [36].

4.2. Hazard

The hazard parameters used in this study reflect the most common triggers for failure, i.e., mass entering a lake, the stability of the terminal moraine, and a buried ice core. Other triggering mechanisms that are commonly included in other studies are seismic activity, extreme temperature/precipitation, and remediation efforts [56]. This study does not address seismic activity or extreme temperature/precipitation because these triggering mechanisms are inherently captured by the other hazard parameters, e.g., extreme temperature/precipitation will alter the hydrostatic pressure on the moraine, so they will be more likely to trigger the failure of an unstable moraine compared to a stable one. Remediation efforts are also not considered in this study because the two lake lowering efforts that were conducted at Tsho Rolpa [10] and Imja Tsho [57] do not influence the results, since the GDEM was created after Tsho Rolpa was lowered and the change in lake level of 3 m at Imja Tsho is within the uncertainty of the GDEM and would not reveal a noticeable change in area from the Landsat imagery.

One difficulty associated with any hazard assessment is developing the best method to translate the parameters into a hazard classification. This is particularly problematic, since GLOFs are unpredictable and often occur in remote locations, so knowledge of previous causes and triggers is limited. Further complicating the issue is that GLOFs can commonly be caused by multiple triggers. Falatkova (Figure 1, 2016) [4] illustrates this issue as dam destabilization and moraine collapse may be caused by an avalanche, increased hydrostatic pressure, buried ice melting, and/or the effect of time. Similarly, Emmer and Cochachin (2013) [3] combine the triggers of hydraulic pressure, buried ice, and the effect of time into one parameter called self-destruction. The combination of GLOF triggers is also inherently embedded in Fujita et al. (2013) [28], which focuses on the breach of the moraine regardless

of the triggering mechanism. A good example of this is the threshold selection of 10° for moraine stability was derived from previous GLOFs, which included at least one GLOF that was triggered by an avalanche (Dig Tsho).

These studies illustrate that while the common triggers are understood, there is still much uncertainty with respect to how these triggering mechanisms interact with one another, and how this can affect the hazard. This uncertainty makes it difficult to quantitatively assess the hazard by assigning weights or values to each parameter, e.g., Bolch et al. (2011) [48] or Wang et al. (2013) [58], since the number of GLOFs that are caused by specific triggers varies between studies, and the cause of many GLOFs is unknown or they could have been caused by a combination of triggers. Rounce et al. (2016) [29] updated all the previously used hazard parameters from the literature [56] to develop a new method, which we assume is best-suited to capture the various triggering mechanisms and/or potential combinations such that the classifications can reflect the most hazardous situations based on previous failures of glacial lakes in the Himalayas. The modifications were made to reflect the most common triggering mechanisms (see Methods).

Lake expansion was also included as part of the hazard assessment to determine how a lake's expansion may alter its proximity to hazards. Surprisingly, given the large growth rates that glacial lakes in Nepal are experiencing (Table 1), lake expansion only altered the hazard classification of one glacial lake. One possible explanation may be that the lack of accuracy in mapping debris-covered glaciers and modeling their ice thickness at the glacier level may be hindering our ability to model future lake extents. Specifically, the lake expansion model predicts that 15 of the 22 glacial lakes that experienced significant growth do not have the ability to continue to grow. However, it is possible that this lack of expansion is an artifact of the model, and some of these lakes may actually continue to grow. These 15 lakes should continue to be monitored in the near future to determine which is correct. Fortunately, the lack of major changes to hazard within the next 15–30 years suggests that ~15 years may be a good interval to update the hazard assessment as this should provide adequate time to include newly formed lakes and revise the hazard assessments for lakes that have grown significantly. However, the hazard assessment would benefit greatly from being updated when high-resolution DEMs become available over the entire study area as this has the potential to greatly improve avalanche and landslide trajectories as well as moraine stability calculations. Once a series of high-resolution DEMs becomes available, DEM differencing could assist the identification of ice-cored moraines, which would experience surface lowering. In the interim period between hazard assessments, resources should be directed towards field assessments and modeling efforts of priority lakes.

4.3. Downstream Impacts

The extent of the GLOF from each lake was conservatively estimated using the MC-LCP model [49] such that the number of hydropower systems, buildings, agricultural land, and bridges located within the flood path could be quantified. The benefit of the MC-LCP model is that it is computationally inexpensive, which allows it to be applied on the large scale. Unfortunately, the model is unable to account for any variations in the PFV of the GLOF because this would require a hydrodynamic model. The use of the MC-LCP model with the GDEM was selected by Rounce et al. (2016) [29] because the model generated a conservative flood extent compared to the flood extent from Dig Tsho [49] and the modeled flood extent from Imja Tsho [45]. It is important to note that these GLOFs had flood volumes of 5 mcm [8] and 33.5 mcm [45], respectively. Therefore, the MC-LCP model is automatically generating flood extents that are associated with large flood volumes regardless of the PFV. A good example of this is the flood extent of Tsho Rolpa and Lake 32 are the same, despite them having drastically different PFVs of 66.3 mcm and 2.3 mcm, respectively.

One way to alleviate this issue is to prioritize lakes that have a PFV over a given threshold. Figure 7 shows that the number of lakes with a given PFV greatly decreases after 2–3 mcm. Previous GLOFs from Dig Tsho in 1985 [8] and Tam Pokhari in 1998 [9] reveal that flood volumes of 5 mcm can have severe socio-economic consequences downstream. Conversely, a glacier outburst flood from Lhotse

Glacier in 2016 that had an estimated flood volume of 2.5 mcm caused minor damage to an outhouse and a bridge, but was primarily confined to the pre-existing channel [59]. If these outburst floods are used as a guide, a threshold of 3 mcm might assist the prioritization of the glacial lakes that should be the immediate concern. The application of physically-based hydrodynamic models for a variety of flood volumes (e.g., Somos-Valenzuela et al., 2015 [45]) performed at multiple lakes would provide useful information for robustly defining a threshold.

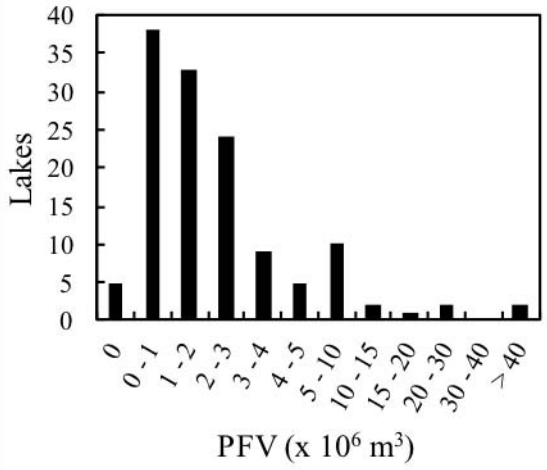

Figure 7. Distribution of potential flood volume (PFV) for all lakes.

These hydrodynamic models would also help determine the threshold for the cutoff distance downstream, which is important for quantifying the downstream impacts. A good example of this is Chamlang North Tsho, which Rounce et al. (2016) [29] found could potentially inundate 244 buildings, 2.5 km^2 of agricultural land, and 14 bridges, compared to this study, which found it could inundate 4 buildings, 0.03 km^2 of agricultural land, and 3 bridges. The drastic change in the downstream impacts is due to the 50 km threshold. This study assumes that beyond 50 km, the wave height is relatively small, e.g., the 2 m wave 200 km from Luggye Tsho [1,51], compared to the surrounding buildings, which are typically located outside of the main river channel. Ideally, hydrodynamic models could be used to quantify the downstream attenuation of the GLOF, which could potentially be incorporated into the MC-LCP model through a cost function based on the downstream distance. Additionally, improved mapping of the locations of existing and proposed hydropower systems would assist quantifications of the socio-economic impacts. Nonetheless, this study is able to conservatively estimate the downstream impacts for each lake, which provides valuable information for decision makers and classifying the risk.

4.4. Risk

The risk assessment is meant to assist decision makers in identifying the lakes that require further investigation, especially since stakeholders in Nepal often have limited financial resources. Specifically, the detailed hazard and risk assessment may help guide the lakes that are the focus of future scientific investigation, which should include much needed field assessments and physically-based hydrodynamic modeling in order to validate the remotely sensed based assessments. The stakeholders and the decision makers are ultimately the individuals and organizations that this study is meant to assist; therefore, the framework and classification system has been developed in a manner that can help prioritize the highest risk lakes. At the same time, the hazard parameters and downstream impacts have been developed in a manner that can provide data to assist decision makers who may have an alternative view of how these lakes should be classified. This study has sought to balance economic and social impacts; however, if economic consequences are prioritized, then Tsho Rolpa and Lake 66 appear to be the riskiest lakes since they are classified as high hazard and threaten hydropower

systems. Alternatively, if decision-makers prioritize social impacts, then Lakes 79, Tsho Rolpa, 45, 81, 23, and Dig Tsho would be the riskiest lakes since they are high and very high hazard and potentially impact the largest numbers of buildings.

The framework and classification system used by this study was designed to prioritize the lakes that have the greatest hazard and socio-economic consequences. The use of a minimum PFV of 3 mcm appears to be justified as the larger the flood, the more likely the flood is going to threaten the buildings and hydropower systems that were identified with the geometric flood model. Future work should use physically-based hydrodynamic models to support or reject this threshold. Based on this 3 mcm PFV threshold, Table 3 shows that there are four lakes that are very high risk, eight lakes that are high risk, and 19 lakes that are moderate risk. The four lakes that are very high risk include Phoksundo Tal, Tsho Rolpa, Lake 99, and Lake 89. Phoksundo Tal has the largest PFV of 197.2 mcm due to its large area (4.56 km^2) and its high average SLA angle (29.9°), which is a result of the lake water discharging into a large waterfall. Tsho Rolpa, which is widely considered to be one of the most dangerous lakes in Nepal [23,24,28,29], and was lowered in 1999 to reduce the lake level by 3 m in an effort to reduce its hazard [10], still appears to be one of the most dangerous lakes due to its steep ice-cored moraine and the threat of both an upstream GLOF and a rockfall. Tsho Rolpa would greatly benefit from physical modeling of an upstream GLOF and/or rockfall to determine how these triggers affect the stability of its moraine.

Table 3. Prioritized list of lakes with highest risk with a minimum PFV of 3 mcm (lines denote the different levels of risk). Hazard, downstream impact, and risk classification values refer to low (0); moderate (1); high (2); and very high (3).

This Study ID	Common Name	Latitude (°)	Longitude (°)	Elev (m.a.s.l.)	Area 2015 (km^2)	Hazard	Impact	Risk	PFV (mcm)
86	Phoksundo Tal	82.948	29.196	3644	4.56	3	2	3	197.2
54	Tsho Rolpa	86.477	27.862	4526	1.52	2	3	3	66.3
99	-	82.415	29.754	4668	0.40	3	2	3	10.0
89	-	82.545	29.194	4682	0.33	3	2	3	7.8
21	Chamlang North	86.957	27.784	5218	0.86	3	1	2	29.6
49	Lumding	86.614	27.779	4819	1.18	3	1	2	21.4
22	Chamlang South	86.960	27.755	4952	0.84	3	1	2	9.3
27	-	86.859	27.688	4762	0.28	3	1	2	6.0
29	-	86.644	27.778	5156	0.28	3	1	2	6.0
83	-	84.472	28.663	4097	0.21	1	3	2	4.0
37	-	86.840	27.793	5300	0.21	2	2	2	4.0
59	-	85.169	28.293	4732	0.19	1	3	2	3.6
129	-	81.780	30.128	5009	0.62	1	1	1	18.5
26	-	86.929	27.850	4579	0.47	1	1	1	12.7
92	-	82.424	29.384	4445	0.44	2	1	1	11.6
50	Lumding Teng	86.621	27.790	5141	0.36	1	1	1	8.7
105	-	82.207	29.929	4564	0.31	2	1	1	6.9
90	-	82.564	29.249	4648	0.29	1	2	1	6.3
2	-	88.049	27.545	5028	0.25	2	1	1	5.3
108	-	82.197	29.994	4383	0.25	1	1	1	5.0
9	-	87.777	27.757	4690	0.24	1	1	1	4.8
80	-	83.186	28.958	5086	0.24	1	2	1	4.8
122	-	82.361	29.432	4401	0.23	1	2	1	4.6
43	Hongu 1	86.936	27.838	5217	0.23	2	1	1	4.6
28	West Hongu	86.918	27.833	5346	0.31	1	1	1	4.4
30	-	86.938	27.857	5472	0.20	1	1	1	3.8
11	-	87.779	27.739	4704	0.19	2	1	1	3.4
10	-	87.784	27.745	4796	0.18	2	1	1	3.2
93	-	82.429	29.407	4416	0.18	1	1	1	3.2
94	Jigilya Daha	82.203	29.666	4379	0.17	2	1	1	3.1
53	Thonak Cho	86.681	27.976	4827	0.57	1	2	1	3.0

Other well-studied lakes that are on this list include Chamlang North Tsho, Lumding Tsho, and Chamlang South Tsho, which have high PFVs and are highly hazardous; however, their downstream

impacts are only moderate (Table 3). Physically-based hydrodynamic flood models would greatly improve the quantification of the socio-economic consequences and assist the decision-making process to determine if these lakes should receive risk-mitigation measures. Two notable lakes that did not make the list of lakes that should be prioritized are Thulagi Tsho and Imja Tsho. Table 2 shows the maximum PFV of these lakes is currently 0.7 mcm and 0.4 mcm, respectively. These lakes have been particularly well studied due to their size and their potential very high and high downstream impacts, respectively. The expected expansion of Imja Tsho until 2045 may cause Imja Tsho to be susceptible to avalanches entering the lake in the future; therefore, it will be important to monitor Imja Tsho's growth moving forward.

5. Conclusions

Nepal appears to be entering a period of time where its government is actively trying to reduce the risk associated with these glacial lakes. This study conducted a holistic assessment of the hazard, downstream impacts, and risk associated with 131 glacial lakes in the Nepal Himalaya that were greater than 0.1 km^2, and identified 11 lakes as very high risk and 31 lakes as high risk. The developed framework assesses the hazard and risk, and reflects the most hazardous conditions based on a comprehensive literature review. The proposed method aims to provide an evaluation that is as objective as possible. However, given the current state of knowledge regarding GLOF triggers and modeling, there is an inherent level of subjectiveness that is unavoidable in these first-pass assessments. We recommend using these results to help prioritize the lakes that should be the focus of future field and modeling studies, and suggest that these results be discussed with relevant stakeholders in Nepal such that decisions with respect to prioritizing resources can be made in line with stakeholder interests (e.g., focus on the most hazardous lakes or the lakes with potentially the largest downstream impacts).

We suggest using the potential flood volume associated with self-destructive and dynamic failures to prioritize glacial lakes such that the lakes with a sizeable flood volume and the greatest risk are the focus of future work. Some of the notable lakes that have large potential flood volumes were Phoksundo Tal, Tsho Rolpa, Chamlang North Tsho, Chamlang South Tsho, and Lumding Tsho. Imja Lake was found to be the only lake where its lake expansion changed its future risk from moderate to high as its future proximity makes it susceptible to an avalanche entering the lake. Since the lake expansion only affected two lakes, we recommend repeating the hazard assessment approximately every 15 years; however, lakes that have significantly grown should be monitored between surveys. Additionally, as higher-resolution DEMs become available, we recommend updating the hazard and risk assessment as these DEMs should greatly improve the modeling of mass entering the lake and modeling the stability of the moraines.

Supplementary Materials: The following are available online at www.mdpi.com/2072-4292/9/7/654/s1, Table S1: Hazard parameters, downstream impacts, classifications, and lake data for all lakes included in this study, Table S2: Statistics regarding comparison of lake delineations with previous studies, shapefiles of polygons for 2000 and 2015 lake delineations as well as the MC-LCP model results and instructional material for using the MC-LCP model.

Acknowledgments: The authors would like to thank Koji Fujita for his encouragement and comments to this study, and Yong Nie for his support with comparing glacial lake surveys. The authors would also like to acknowledge the support of the NSF-CNH program (award no. 1516912) for the support of David Rounce and Daene McKinney. The Landsat imagery used in this study was provided by the Land Processes Distributed Active Archive Center (LP DAAC).

Author Contributions: David Rounce and Daene McKinney designed the study. David Rounce carried out the glacial lake survey, hazards modeling, processing and analysis, and Scott Watson carried out the MC-LCP modeling and downstream impacts quantification. David Rounce, Scott Watson, and Daene McKinney wrote the paper.

Conflicts of Interest: The authors declare no conflict of interest.

References

1. Richardson, S.D.; Reynolds, J.M. An overview of glacial hazards in the Himalayas. *Quat. Int.* **2000**, *65/66*, 31–47. [CrossRef]
2. Wang, X.; Yao, T.; Gao, Y.; Yang, X.; Kattel, D.B. A first-order method to identify potentially dangerous glacial lakes in a region of the southeastern Tibetan Plateau. *Mt. Res. Dev.* **2011**, *31*, 122–130. [CrossRef]
3. Emmer, A.; Cochachin, A. The causes and mechanisms of moraine-dammed lake failures in the Cordillera Blanca, North American Cordillera and Himalaya. *AUC Geogr.* **2013**, *48*, 5–15. [CrossRef]
4. Falatkova, K. Temporal analysis of GLOFs in high-mountain regions of Asia and assessment of their causes. *AUC Geogr.* **2016**, *51*, 145–154. [CrossRef]
5. Westoby, M.J.; Glasser, N.F.; Brasington, J.; Hambrey, M.J.; Quincey, D.J.; Reynolds, J.M. Modelling outburst floods from moraine-dammed glacial lakes. *Earth-Sci. Rev.* **2014**, *134*, 137–159. [CrossRef]
6. Carrivick, J.L.; Tweed, F.S. A global assessment of the societal impacts of glacier outburst floods. *Glob. Planet. Chang.* **2016**, *144*, 1–16. [CrossRef]
7. Buchroithner, M.F.; Jentsch, G.; Wanivenhaus, B. Monitoring of recent geological events in the Khumbu area (Himalaya, Nepal) by digital processing of Landsat MSS Data. *Rock Mech.* **1982**, *15*, 181–197. [CrossRef]
8. Vuichard, D.; Zimmermann, M. The 1985 catastrophic drainage of a moraine-dammed lake, Khumbu Himal, Nepal: Cause and consequences. *Mt. Res. Dev.* **1987**, *7*, 91–110. [CrossRef]
9. Osti, R.; Bhattarai, T.N.; Miyake, K. Causes of catastrophic failure of Tam Pokhari moraine dam in the Mt. Everest region. *Nat. Hazards* **2011**, *58*, 1209–1223. [CrossRef]
10. Reynolds, J.M. Glacial hazard assessment at Tsho Rolpa, Rolwaling, Central Nepal. *Q. J. Eng. Geol. Hydrogeol.* **1999**, *32*, 209–214. [CrossRef]
11. Gardelle, J.; Arnaud, Y.; Berthier, E. Contrasted evolution of glacial lakes along the Hindu Kush Himalaya mountain range between 1990 and 2009. *Glob. Planet. Chang.* **2011**, *75*, 47–55. [CrossRef]
12. Nie, Y.; Liu, Q.; Liu, S. Glacial lake expansion in the central Himalayas by Landsat images, 1990–2010. *PLoS ONE* **2013**, *8*, e83973. [CrossRef] [PubMed]
13. Nie, Y.; Sheng, Y.; Liu, Q.; Liu, L.; Liu, S.; Zhang, Y.; Song, C. A regional-scale assessment of Himalayan glacial lake changes using satellite observations from 1990 to 2015. *Remote Sens. Environ.* **2017**, *189*, 1–13. [CrossRef]
14. Song, C.; Sheng, Y.; Wang, J.; Ke, L.; Madson, A.; Nie, Y. Heterogeneous glacial lake changes and links of lake expansions to the rapid thinning of adjacent glacier termini in the Himalayas. *Geomorphology* **2016**, *280*, 30–38. [CrossRef]
15. Benn, D.I.; Bolch, T.; Hands, K.; Gulley, J.; Luckman, A.; Nicholson, L.I.; Quincey, D.; Thompson, S.; Toumi, R.; Wiseman, S. Response of debris-covered glaciers in the Mount Everest region to recent warming, and implications for outburst flood hazards. *Earth-Sci. Rev.* **2012**, *114*, 156–174. [CrossRef]
16. Miles, E.S.; Willis, I.C.; Arnold, N.S.; Steiner, J.; Pellicciotti, F. Spatial, seasonal and interannual variability of supraglacial ponds in the Langtang Valley of Nepal, 1999–2013. *J. Glaciol.* **2016**, *63*, 88–105. [CrossRef]
17. Watson, C.S.; Quincey, D.J.; Carrivick, J.L.; Smith, M.W. The dynamics of supraglacial ponds in the Everest region, central Himalaya. *Glob. Planet. Chang.* **2016**, *142*, 14–27. [CrossRef]
18. Watanabe, T.; Ives, J.D.; Hammond, J.E. Rapid growth of a glacial lake in Khumbu Himal, Himalaya: Prospects for a catastrophic flood. *Mt. Res. Dev.* **1994**, *14*, 329–340. [CrossRef]
19. Thompson, S.S.; Benn, D.I.; Dennis, K.; Luckman, A. A rapidly growing moraine-dammed glacial lake on Ngozumpa Glacier, Nepal. *Geomorphology* **2012**, *145–146*, 1–11. [CrossRef]
20. Thompson, S.; Benn, D.I.; Mertes, J.; Luckman, A. Stagnation and mass loss on a Himalayan debris-covered glacier: Processes, patterns and rates. *J. Glaciol.* **2016**, *62*, 467–485. [CrossRef]
21. Wang, X.; Liu, S.; Ding, Y.; Guo, W.; Jiang, Z.; Lin, J.; Han, Y. An approach for estimating the breach probabilities of moraine-dammed lakes in the Chinese Himalayas using remote-sensing data. *Nat. Hazards Earth Syst. Sci.* **2012**, *12*, 3109–3122. [CrossRef]
22. Petrov, M.A.; Sabitov, T.Y.; Tomashevskaya, I.G.; Glazirin, G.E.; Chernomorets, S.S.; Savernyuk, E.A.; Tutubalina, O.V.; Petrakov, D.A.; Sokolov, L.S.; Dokukin, M.D.; et al. Glacial lake inventory and lake outburst potential in Uzbekistan. *Sci. Total Environ.* **2017**, *592*, 228–242. [CrossRef] [PubMed]

23. Mool, P.K.; Bajracharya, S.R.; Joshi, S.P. *Inventory of Glaciers, Glacial Lakes and Glacial Lake Outburst Floods, Nepal*; International Centre for Integrated Mountain Development (ICIMOD): Kathmandu, Nepal, 2001; Volume 363.
24. International Centre for Integrated Mountain Development (ICIMOD). *Glacial Lakes and Glacial Lake Outburst Floods in Nepal*; ICIMOD: Kathmandu, Nepal, 2011.
25. Mool, P.K.; Wangda, D.; Bajracharya, S.R.; Kunzang, K.; Gurung, D.R.; Joshi, S.P. *Inventory of Glaciers, Glacial Lakes and Glacial Lake Outburst Floods, Bhutan*; International Centre for Integrated Mountain Development (ICIMOD): Kathmandu, Nepal, 2001; Volume 227.
26. Worni, R.; Huggel, C.; Stoffel, M. Glacial lakes in the Indian Himalayas from an area-wide glacial lake inventory to on-site and modeling based risk assessment of critical glacial lakes. *Sci. Total Environ.* **2013**, *468–469*, S71–S84. [CrossRef] [PubMed]
27. Allen, S.K.; Linsbauer, A.; Randhawa, S.S.; Huggel, C.; Rana, P.; Kumari, A. Glacial lake outburst flood risk in Himachal Pradesh, India: An integrative and anticipatory approach considering current and future threats. *Nat. Hazards* **2015**, 1741–1763. [CrossRef]
28. Fujita, K.; Sakai, A.; Takenaka, S.; Nuimura, T.; Surazakov, A.B.; Sawagaki, T.; Yamanokuchi, T. Potential flood volume of Himalayan glacial lakes. *Nat. Hazards Earth Syst. Sci.* **2012**, *13*, 1827–1839. [CrossRef]
29. Rounce, D.R.; McKinney, D.C.; Lala, J.M.; Byers, A.C.; Watson, C.S. A new remote hazard and risk assessment framework for glacial lakes in the Nepal Himalaya. *Hydrol. Earth Syst. Sci.* **2016**, *20*, 3455–3475. [CrossRef]
30. McFeeters, S.K. The use of the normalized difference water index (NDWI) in the delineation of open water features. *Int. J. Remote Sens.* **1996**, *17*, 1425–1432. [CrossRef]
31. Bolch, T.; Buchroithner, M.F.; Peters, J.; Baessler, M.; Bajracharya, S. Identification of glacier motion and potentially dangerous glacial lakes in the Mt. Everest region/Nepal using spaceborne imagery. *Nat. Hazards Earth Syst. Sci.* **2008**, *8*, 1329–1340. [CrossRef]
32. Fujita, K.; Sakai, A.; Nuimura, T.; Yamaguchi, S.; Sharma, R.R. Recent changes in Imja Glacial Lake and its damming moraine in the Nepal Himalaya revealed by in-situ surveys and multi-temporal ASTER imagery. *Environ. Res. Lett.* **2009**, *4*, 045205. [CrossRef]
33. Frey, H.; Machguth, H.; Huss, M.; Huggel, C.; Bajracharya, S.; Bolch, T.; Kulkarni, A.; Linsbauer, A.; Salzmann, N.; Stoffel, M. Estimating the volume of glaciers in the Himalayan-Karakoram region using different methods. *Cryosphere* **2014**, *8*, 2313–2333. [CrossRef]
34. Linsbauer, A.; Frey, H.; Haeberli, W.; Machguth, H.; Azam, M.F.; Allen, S. Modelling glacier-bed overdeepenings and possible future lakes for the glaciers in the Himalaya-Karakoram region. *Ann. Glaciol.* **2016**, *57*, 119–130. [CrossRef]
35. Nuimura, T.; Sakai, A.; Taniguchi, K.; Nagai, H.; Lamsal, D.; Tsutaki, S.; Kozawa, A.; Hoshina, Y.; Takenaka, S.; Omiya, S.; et al. The GAMDAM glacier inventory: A quality controlled inventory of Asian glaciers. *Cryosphere* **2015**, *9*, 849–864. [CrossRef]
36. Paul, F.; Barrand, N.E.; Baumann, S.; Berthier, E.; Bolch, T.; Casey, K.; Frey, H.; Joshi, S.P.; Konovalov, V.; Bris, R.LE.; et al. On the accuracy of glacier outlines derived from remote-sensing data. *Ann. Glaciol.* **2013**, *54*, 171–182. [CrossRef]
37. Arendt, A.; Bliss, A.; Bolch, T.; Cogley, J.G.; Gardner, A.S.; Hagen, J.-O.; Hock, R.; Huss, M.; Kaser, G.; Kienholz, C.; et al. Randolph Glacier Inventory—A Dataset of Global Glacier Outlines: Version 5.0. In *Global Land Ice Measurements from Space*; Digital Media: Boulder, CO, USA, 2015.
38. Yamada, T. *Glacier Lake and Its Outburst Flood in the Nepal Himalaya*; Japanase Society of Snow and Ice: Tokyo, Japan, 1998; pp. 1–96.
39. ASTER GDEM Validation Team. ASTER Global Digital Elevation Model Version 2 Summary of Validation Results. 2011. Available online: https://lpdaacaster.cr.usgs.gov/GDEM/Summary_GDEM2_validation_report_final.pdf (access on 1 February 2015).
40. Alean, J. Ice avalanches: Some empirical information about their formation and reach. *J. Glaciol.* **1985**, *31*, 324–333. [CrossRef]
41. Shea, J.M.; Immerzeel, W.W.; Wagnon, P.; Vincent, C.; Bajracharya, S. Modelling glacier change in the Everest region, Nepal Himalaya. *Cryosphere* **2015**, *9*, 1105–1128. [CrossRef]
42. Huggel, C.; Haeberli, W.; Kääb, A.; Bieri, D.; Richardson, S. An assessment procedure for glacial hazards in the Swiss Alps. *Can. Geotech. J.* **2004**, *41*, 1068–1083. [CrossRef]

43. Huggel, C.; Zgraggen-Oswald, S.; Haeberli, W.; Kääb, A.; Polkvoj, A.; Galushkin, I.; Evans, S.G. The 2002 rock/ice avalanche at Kolka/Karmadon, Russian Caucasus: Assessment of extraordinary avalanche formation and mobility, and application of Quick-Bird satellite imagery. *Nat. Hazards Earth Syst. Sci.* **2005**, *5*, 173–187. [CrossRef]
44. Worni, R.; Huggel, C.; Clague, J.J.; Schaub, Y.; Stoffel, M. Coupling glacial lake impact, dam breach, and flood processes: A modeling perspective. *Geomorphology* **2014**, *224*, 161–176. [CrossRef]
45. Somos-Valenzuela, M.A.; Chisolm, R.E.; Rivas, D.S.; Portocarrero, C.; McKinney, D.C. Modeling a glacial lake outburst flood process chain: The case of Lake Palcacocha and Huaraz, Peru. *Hydrol. Earth Syst. Sci.* **2016**, *20*, 2519–2543. [CrossRef]
46. Bolch, T.; Peters, J.; Yegorov, A.; Pradhan, B.; Buchroithner, M.; Blagoveshchensky, V. Identification of potentially dangerous glacial lakes in the northern Tien Shan. *Nat. Hazards* **2011**, *59*, 1691–1714. [CrossRef]
47. Dahal, R.K.; Hasegawa, S.; Nonomura, A.; Yamanaka, M.; Dhakal, S.; Paudyal, P. Predictive modelling of rainfall-induced landslide hazard in the Lesser Himalaya of Nepal based on weights-of-evidence. *Geomorphology* **2008**, *102*, 496–510. [CrossRef]
48. Collins, B.D.; Gibson, R.W. *Assessment of Existing and Potential Landslide Hazards Resulting from the April 25, 2015 Gorkha, Nepal Earthquake Sequence*; Open-File Report 2015-1142; U.S. Geological Survey: Reston, VI, USA, 2015.
49. Watson, C.S.; Carrivick, J.; Quincey, D. An improved method to represent DEM uncertainty in glacial lake outburst flood propagation using stochastic simulations. *J. Hydrol.* **2015**, *529*, 1373–1389. [CrossRef]
50. Somos-Valenzuela, M.A.; McKinney, D.C.; Byers, A.C.; Rounce, D.R.; Portocarrero, C.; Lamsal, D. Assessing downstream flood impacts due to a potential GLOF from Imja Tsho in Nepal. *Hydrol. Earth Syst. Sci.* **2015**, *19*, 1401–1412. [CrossRef]
51. Reynolds, J.M. Assessing glacial hazards for hydro development in the Himalayas, Hindu Kush and Karakoram. *Hydropower Dams* **2014**, *2*, 60–65.
52. Uddin, K.; Shrestha, H.L.; Murthy, M.S.R.; Bajracharya, B.; Shrestha, B.; Gilani, H.; Pradhan, S.; Dangol, B. Development of 2010 national land cover database for the Nepal. *J. Environ. Manag.* **2015**, *148*, 82–90. [CrossRef] [PubMed]
53. Garrard, R.; Kohler, T.; Price, M.F.; Byers, A.C.; Sherpa, A.R.; Maharjan, G.R. Land use and land cover change in Sagarmatha National Park, a World Heritage Site in the Himalayas of eastern Nepal. *Mt. Res. Dev.* **2016**, *36*, 299–310. [CrossRef]
54. Huggel, C.; Kääb, A.; Haeberli, W.; Teysseire, P.; Paul, F. Remote sensing based assessment of hazards from glacier lake outbursts: A case study in the Swiss Alps. *Can. Geotech. J.* **2002**, *39*, 316–330. [CrossRef]
55. Cook, S.J.; Quincey, D.J. Estimating the volume of Alpine glacial lakes. *Earth Surf. Dyn.* **2015**, *3*, 559–575. [CrossRef]
56. Emmer, A.; Vilímek, V. Review article: Lake and breach hazard assessment for moraine-dammed lakes: An example from the Cordillera Blanca (Peru). *Nat. Hazards Earth Syst. Sci.* **2013**, *13*, 1551–1565. [CrossRef]
57. United Nations Development Programme (UNDP). *Community Based Glacier Lake Outburst and Flood Risk Reduction in Nepal*; Project Document; UNDP Environmental Finance Services: Kathmandu, Nepal, 2013.
58. Wang, X.; Ding, Y.; Liu, S.; Jiang, L.; Wu, K.; Jiang, Z.; Guo, W. Changes of glacial lakes and implications in Tian Shan, central Asia, based on remote sensing data from 1990 to 2010. *Environ. Res. Lett.* **2013**, *8*, 044052. [CrossRef]
59. Rounce, D.R.; Byers, A.C.; Byers, E.A.; McKinney, D.C. Brief communication: Observations of a glacier outburst flood from Lhotse Glacier, Everest Area, Nepal. *Cryosphere* **2017**, *11*, 443–449. [CrossRef]

© 2017 by the authors. Licensee MDPI, Basel, Switzerland. This article is an open access article distributed under the terms and conditions of the Creative Commons Attribution (CC BY) license (http://creativecommons.org/licenses/by/4.0/).